Analyst

PAPER

View Article Online
View Journal

Cite this: DOI: 10.1039/c5an00364d

A microfluidic immunoassay platform for the detection of free prostate specific antigen: a systematic and quantitative approach†

Narayanan Madaboosi,‡[a] Ruben R. G. Soares,‡[a,b] Virginia Chu[a] and João Pedro Conde*[a,c]

Received 24th February 2015,
Accepted 1st May 2015

DOI: 10.1039/c5an00364d

www.rsc.org/analyst

As a leading cause of cancer-related deaths in men globally, prostate cancer (PCa) demands immense attention for theranostic purposes. There is an increasing need for the development of rapid, sensitive, economical, miniaturized and multiplexable assays. Towards this goal, we present a systematic approach for the optimisation of a microfluidic sandwich immunoassay, which can be applied as a generic biosensor platform for PCa detection. Prostate specific antigen (PSA) was used as the model biomarker, and its free form was captured using commercially available antibodies and detected using chemiluminescence, both in spiked buffer and matrix solutions. Along with the optimisation of surface chemistry and microfluidic parameters, we report a bio-affinity amplification strategy based on biotin–streptavidin chemistry to bring the limits of detection for free-PSA from 21.4 ng mL^{-1} down to 2.7 ng mL^{-1}, within the clinically relevant range. An estimate of the surface coverage and simulations of the interactions taking place in the microfluidic biosensor during the assay are also presented. This novel platform using a simple passive adsorption-based bio-affinity strategy, when coupled with multiplexing and integrated detection, can serve as a promising point-of-care diagnostic tool for PCa.

Introduction

In the clinical and biomedical arenas, there is an urgent need for accurate diagnosis and prognosis of prostate cancer (PCa). In the West, PCa is the most common non-cutaneous malignancy and the second most common cause of cancer-related deaths among men.[1] PCa in either its aggressive or indolent forms demands diagnostic accuracy[2] to ensure proper treatment or to avoid overtreatment, respectively. For this purpose, PCa biomarkers and their quantification become relevant.

PSA, an androgen-regulated 33 kDa serine protease (kallikrein-3) secreted by the epithelial cells of the prostate, was approved by the US FDA in 1986 for PCa monitoring and later in 1994 for widespread screening, thus becoming the foundation of early PCa detection and management.[3] However, although PSA is currently the golden standard for PCa diagnosis and has revolutionized the way PCa is diagnosed and treated around the world, it is not without its drawbacks among which include false positives due to elevated PSA levels from non-cancerous prostatitis, benign prostate hyperplasia (BPH) or diet alterations and an inability to distinguish between stages of PCa. Refinements to PSA tests, aimed at improving the operating characteristics of PSA-based assays, such as total PSA (tPSA) (sum of free unbound PSA (fPSA) and bound PSA complexed predominantly to the α-1-antichymotrypsin (PSA-ACT)) assay,[4] percentage free PSA test (allowing discrimination between PCa and BPH),[5] equimolar tPSA assay (measurement of immunologically detectable forms of PSA on an equimolar basis to avoid preferential detection of fPSA)[6] and prostate health index (calculated from a combination of tPSA, fPSA and a truncated PSA isoform)[7] drive the PSA measurements, especially in the 'gray zone' (4–10 ng mL^{-1}), to the roads of effective PCa diagnosis and treatment. The measurement of fPSA becomes essential for calculating all of the above-mentioned values, thus underlining the significance of its accurate quantification.

Classical PSA quantification for clinical tests is based on the microtitre plate enzyme linked immunosorbent assay (ELISA). These assays have long incubation times, voluminous use of reagents, need for trained personnel and difficulty in implementing at point-of-care.[8,9] At the other end, lateral flow

[a]INESC Microsistemas e Nanotecnologias (INESC MN) and IN – Institute of Nanoscience and Nanotechnology, Lisbon, Portugal. E-mail: joao.conde@tecnico.ulisboa.pt
[b]iBB – Institute for Bioengineering and Biosciences, Instituto Superior Técnico, Universidade de Lisboa, Lisbon, Portugal
[c]Department of Bioengineering, Instituto Superior Técnico, Universidade de Lisboa, Lisbon, Portugal
†Electronic supplementary information (ESI) available. See DOI: 10.1039/c5an00364d
‡Equal contribution.

based assays, based on colorimetry[10] or fluorescence,[11] suffer from quantitative limitations, thus widely remaining qualitative.[12] Modified methods such as nanoparticle based time-resolved fluorescence, multianalyte ELISA and microcantilever assays involve complexities like particle modification steps, large microtitre plate volumes and complex equipment, respectively.[13–15] In this context, microfluidics offers advantages such as economy of reagents, shorter analysis times, precise control over the concentration of molecules both in space and time, higher analysis throughput, ease for integration and portability for point-of-care (PoC) measurements, amongst others.[16] With these benefits, microfluidics-based biosensors hold promise for biomedical research, in general[17] and future PoC cancer diagnosis, in particular.[18]

Antibody (Ab)-based biosensors have transformed diagnostics in PoC clinical settings, including for PSA.[19,20] However, previous studies targeting the detection of PSA using microfluidic immunoassays either required extra processing of preparatory components,[21,22] complex integrated units, massive external read-out systems[23] or stringent surface chemistry such as covalent modification.[24] Other studies aiming to detect related cancer biomarkers like IL-6 required the use of an external magnetic field, covalent surface modification, *etc.*[25,26] Results indicating that Ab immobilisation *via* an appropriate physical adsorption can effectively replace the more complex processes involved in covalent immobilisation provide motivation for a simpler assay.[27] In this work, we exploit the streptavidin–biotin chemistry, based on the extremely high affinity of streptavidin towards biotin (dissociation constant (K_d) of 4×10^{-14} M). Each streptavidin has the ability to bind four biotin molecules and the bond is formed rapidly, thus proving advantageous for the short interaction times desired in microfluidics and once formed it is unaffected by extremes of temperature, pH and even denaturing agents; also, such a combination yields convincingly good signals when conjugated with chemiluminescent tags like horseradish peroxidase (HRP) or alkaline phosphatase.[13,28,29] Based on this, we took advantage of building a network of streptavidin–biotin molecules, linked suitably to the antibodies, in order to amplify the signal in the assay system.

As a whole, surface chemistry and its modification play a key role in deciding the efficacy of any biosensor based immunoassay.[30] Knowledge about relative surface coverage and Ab orientation on one hand,[31,32] and the transport of molecules to the sensor surface and binding equilibrium on the other hand[33] are key to optimising sensitivity and specificity. This means that the over-all performance of an immunosensor results from a multi-parametric system ranging from surface functionalization, Ab orientation and density on the sensor[34] to analyte delivery, washing and detection.[35] For these reasons, a careful and clear optimisation of these parameters needs to be performed for validation of the immunosensor. Although there are studies in the literature reporting the effect of different parameters on microfluidic immunoassays, a systematic approach simultaneously delineating and integrating the effects of the surface, microfluidic as well as immunological parameters, the tailoring of which leads to an enhancement in the sensitivity, is novel. In this work, we present a microfluidic sandwich immunoassay for fPSA detection by systematically analyzing the critical components of the immunoassay based on simple passive adsorption only and achieve a ten-fold decrease in the limits of detection (LoD) using the bio-affinity amplification based on streptavidin–biotin chemistry.

Methods

Fabrication of PDMS microchannels

The polydimethylsiloxane (PDMS) microfluidic structures were fabricated using a soft lithography process. The process for the fabrication of the lithography mask, the SU-8 mold and the PDMS structures is described elsewhere (Soares *et al.*, 2014).[36] In summary, the patterns of an aluminium mask were lithographically transferred to SU-8 (Microchem, Newton, USA), a negative photoresist with UV exposure and development in propylene glycol monomethyl ether acetate (Sigma-Aldrich, Portugal). The patterned SU-8 serves as a mould for the subsequent reproduction of structures in PDMS. The PDMS structure (with microchannel width, w = 200 μm, height, h = 20 μm and length, l = 1 cm) and the cleaned glass substrate were sealed by subjecting both of them to UV-ozone treatment for 6 min at 28–32 mW cm^{-2} (UVO cleaner 144AX, Jelight Company Inc., CA, USA) for surface oxidation. The surface oxidized PDMS and glass substrates were then brought together and gently pressed to ensure bonding. After a day, the microfluidic devices are permanently sealed and ready to be used for the immunoassays. For nanospotting experiments, the sealing was done by exposing the PDMS device containing the microfluidic structures, opened to air, to a hand-held corona discharge generator (Corona Treater BD20AC, Electro-Technic Products, IL, USA) for 30–45 s at a distance of about 0.5 cm to make their surfaces hydrophilic.

Microfluidic sandwich immunoassays

Phosphate buffered saline (PBS) tablets (P4417), human serum albumin (HSA) (A9511), bovine serum albumin (A2153), biotin labelled bovine albumin (Biotin-BSA) (A8549), streptavidin (S4762), mouse IgG (I5381), rabbit IgG (I5006), goat IgG (I5256), rabbit anti-mouse IgG-horseradish peroxidase (HRP) (A9044), goat anti-rabbit IgG-HRP (A6154), rabbit anti-goat IgG-HRP (A5420), and goat anti-mouse IgG-fluorescein isothiocyanate (FITC) (F0257) were all purchased from Sigma-Aldrich, Portugal. BSA-FITC (A23015), streptavidin-FITC (SNN1008), and streptavidin-HRP were purchased from Invitrogen Life Technologies (MA, USA). PSA from human semen (30C-CP1017P) was obtained from Fitzgerald (MA, USA). Luminol, Pierce (SuperSignal® West Femto Substrate Trial Kit 34094 and SuperSignal West Pico 35065) was used as purchased from Thermo Scientific, Portugal. IL-6 protein (ab101044) was obtained from Abcam (Cambridge, UK). In addition, the set of antibodies were also purchased from Abcam (Table 1).

The solutions were prepared using ultrapure water, obtained using a MilliQ purification system from Millipore

Table 1 List and description of PSA-specific and other antibodies used in the study

Product	Catalogue no.	Epitope	Remarks
Anti-PSA Ab [8A6]	Ab10187	1	Used as capture Ab for fPSA assays
Anti-PSA Ab [PS2]	Ab10189	3	Used as capture Ab for both fPSA and equimolar total (emt)-PSA assays
Anti-PSA Ab [5A6]	Ab10185	5	Used as capture Ab for both fPSA and emt-PSA assays
Anti-PSA Ab [5A6]-HRP	Ab24466	5	Used as a detector Ab for chemiluminescence-based PSA assays
Anti-PSA Ab [5A6]-FITC	Ab178776	5	Used as a detector Ab for fluorescence-based PSA assays
Anti-PSA Ab [PS2]-Biotin	Ab182030	3	Biotinylated Ab used in amplification PSA assays with Ab10187/85 as capture Ab
Anti-PSA Ab [5A6]-Biotin	Ab182031	5	Biotinylated Ab used in amplification PSA assays with Ab10187/89 as capture Ab
Anti-PSA Ab	Ab76113	—	PSA specific rabbit monoclonal Ab
Anti-IL6 Ab	Ab9324	—	Mouse monoclonal used as capture Ab for IL6 specificity control assays
Anti-IL6 Ab-Biotin	Ab84251	—	Rabbit polyclonal used as detector Ab for IL6 specificity control assays

(MA, USA). All the antibodies were diluted in PBS filtered through a 0.2 μm syringe filter (Whatman GmbH, Germany). Metallic plug adapters for the microchannel and capillary tubing (BTPE-90) were purchased from Instech Solomon (PA, USA). 1 mL syringes were from CODAN, Germany. The liquid flow in the microchannel was controlled using a NE-300 syringe pump from New Era (NY, USA).

The individual schemes for the sandwich assays are explained along with the figures. Briefly, as described by Madaboosi *et al.*,[37] the capture Ab was adsorbed on the channel, followed by blocking with 4% (w/v) BSA diluted in PBS, then flowing the PSA spiked solutions and finally the detector Ab. Suitable modifications are made when the biotin–streptavidin combination is used for amplification-based experiments. Unless mentioned, the reagents were flowed at a rate of (Q) = 0.5 μL min^{-1} for 10 min, and PBS for rinsing at Q = 5 μL min^{-1} for 1 min. For luminol, Q = 5 μL min^{-1} was used as well. The capture and detector Abs were used at a concentration of 100 μg mL^{-1}, streptavidin also at a concentration of 100 μg mL^{-1}, biotin-BSA at a concentration of 200 μg mL^{-1} and streptavidin-HRP at 100 μg mL^{-1}.

Nanospotting of antibodies in PDMS microchannels

The mouse IgG and Ab10187 antibodies were spotted on PDMS microchannel surfaces as detailed by Novo *et al.*[38] A non-contact spotter (Nanoplotter NP2.1, GeSiM, Germany) was used to spot the Ab solutions with a piezoelectric pipette (with a capacity to dispense single droplets with volumes down to ~56 pL) mounted on a computer controlled stage, allowing the precise alignment of the spot inside the microchannel. The total number of times a droplet solution was dispensed at a particular location determines the diameter and the amount of Ab at that spot. The temperature was fixed at 16 °C and humidity was adjusted to near the dew point to increase the evaporation time of the droplets, ensuring homogeneous drying.

Image acquisition and analysis

A fluorescence microscope (Leica DMLM) connected to a digital camera (Leica DFC300FX) was used for imaging the microchannels and recording the signal. Optical micrographs of the fluorescence signal from the microchannels were obtained with an exposure time of 1 s and 2× optical gain. The chemiluminescence signal was recorded with an exposure time of 10 s and 10× optical gain, all in a dark background. The acquired images were analysed using ImageJ software (National Institutes of Health, USA). The values correspond to the average measurements from three independent experiments, and with three regions of interest in each of the experiments, after subtraction of the background signal.

Results and discussion

The control of the surface chemistry in the microchannels is shown *via* generic Ab measurements on the treated surface. Nanospotting experiments are used to validate these measurements by allowing a correlation of the measured signals with those obtained using known quantities of PSA-specific antibodies. After analyzing the surface characteristics, a systematic study of the other assay parameters such as microfluidic conditions (flow rate, incubation time, rinsing, *etc.*), specificity tests using relevant antibodies, together with the needed immunological controls, and the proof-of-concept for a PSA measurement in matrix solution are presented. Measurements with fPSA, with and without amplification, highlight the need for a bio-affinity based strategy to bring down the LoD towards the clinical regime. Finally, a theoretical note on the parameters influencing the control over the molecular interactions in the microchannel on the surface and the binding kinetics is added, acting as a complement to validate this systematic approach and provide insights over the physical and chemical aspects governing the assay.

Terminologies and concepts

The experiments were performed in a microfluidic channel and fluorescence mode of detection was used for the studies helping to understand the surface chemistry and other optimisation experiments. The dimensions of the microchannel used and the terminologies for the relevant microfluidic as well as surface characteristics to be discussed in the later sections are listed and described in Table 2.

Briefly, for a sandwich assay that has been optimized in this work, 'probe' refers to the capture Ab molecule that is

Table 2 Optimisation and associated assay conditions for fPSA detection

Parameter	Value	Notes
(a) Channel dimensions		Relates to the dimensions of the microchannel
W_c	200 μm	Width
H	20 μm	Height
(b) Dimensions of the sensing area		Relates to the effective area of the channel functionalized with probe molecules
W_s	200 μm	Width
L	3000 μm	Length
λ	150	Aspect ratio (L/H)
(c) Surface coverage		Defines the interaction between the incoming analyte molecules and the available probes
b_m	1.5×10^{11} cm^{-2}	Probe surface density
N_R	9×10^8	Effective number of probes bound to the surface
K_d	1.75×10^{-8} M	Dissociation constant, relating to the binding (k_{on}) and unbinding (k_{off}) events of the analyte with the probe (Ab10185)
(d) Assay conditions		Defines the microfluidic conditions optimized in order to perform the fPSA assay
C_o	38 pM to 38 nM	Initial analyte concentration flowing through the microchannel (1–1000 ng mL^{-1} PSA)
Q	0.5 μL min^{-1}	Flow rate inside the microchannel
t	10 min	Time of incubation of the molecules in the microchannel
D	8.5×10^{-7} cm^2 s^{-1}	Diffusion coefficient of the analyte in solution
M_W	26 079 Da	Molecular weight of the analyte[39]
Re	0.076	Reynolds number (≪1, laminar flow conditions)

immobilised on the surface, 'analyte' is the protein of interest, fPSA in this case, that is being captured by the immobilised probe and 'detector' is another Ab molecule that is specific to an epitope, different from the one that is recognized by the capture antibody, usually tagged with a fluorescent or chemiluminescent label, enabling microscopic detection. The optimisation experiments are done using generic mouse or goat anti-IgG antibodies, the conditions of which are extrapolated to PSA specific antibodies in the study. 'Blocking' refers to steps where non-PSA protein molecules like BSA are used to fill-in the empty regions of the microchannel after the previous probe adsorption step, in order to decrease the signal emerging from non-specific adsorption. 'Washing' refers to the flowing of PBS inside the microchannel, usually done intermittently between every individual step of the immunoassay, and also after the final step (usually to remove the unbound and loosely bound molecules from the surface).

Control over surface chemistry

Concentration of the immobilisation probe. First, the concentration of immobilised Ab is optimised to saturate the surface, so that the probe density on the surface can be estimated. To find the optimal conditions to allow the saturation of the substrate in the PDMS structure (also ensuring surface coverage as a monolayer, reproducible between experiments), two approaches were used: (i) a direct measurement, where FITC-labelled α-mouse IgGs were flowed at various concentrations, and (ii) an indirect measurement, where unlabelled α-mouse IgGs were first flowed and the surface saturation was indirectly measured by flowing FITC-labelled BSA. In the former case, the amplitude of the signal obtained directly correlates with the surface covered by the labelled antibodies and in the latter case, the signal is inversely proportional to the surface covered by the antibodies (the reason being the higher the number of Ab molecules that cover the surface, the lower the number of labelled BSA molecules that can bind to the free space and vice-versa). The results for both the direct and indirect measurements are shown in Fig. 1. It can be observed that the signal from the direct measurement increases with the Ab concentration, while that for the indirect measurement decreases.

The different possible orientations of Abs and the influence of concentration not only on their adsorption but also on the assay underline the need for optimizing the concentration for an immunoassay.[32] In this context, from Fig. 1, an Ab concentration of 100 μg mL^{-1} would yield a surface completely saturated with Abs, as above this level the curve reaches a plateau. The use of concentrations of probe molecules above the saturation point could result in coverage in excess of a monolayer and there are reports that suggest that in this situation Abs adsorb onto and block others on the surface, rendering their binding sites less accessible.[31] Hence, to remain in the regime where such a masking effect does not occur and simultaneously ensuring adequate probe coverage for analyte binding, we choose 100 μg mL^{-1} as the probe concentration for the assays. As orientation is a function of surface coverage and can also significantly improve the analyte binding signal,

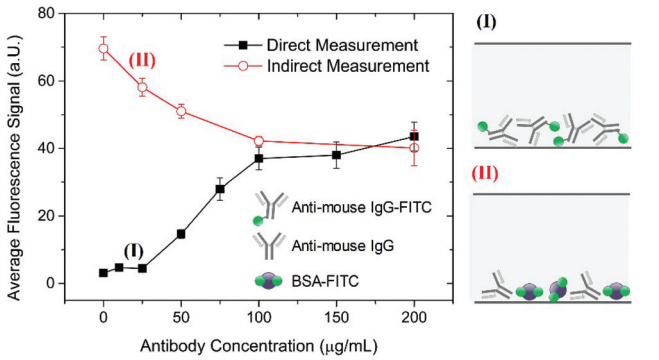

Fig. 1 Optimisation of the surface concentration of immobilisation antibodies for the immunoassay. Filled squares show values from direct measurements, where the FITC-labelled IgGs are directly adsorbed on the surface, and open circles show values from indirect measurements, where unlabelled IgGs are first adsorbed on the surface and then measured using FITC labelled BSA. The schematics for the assay are also given as an inset. It can be noted that the signal from the surface saturates with 100 μg mL^{-1} of the antibody concentration.

the capture antibody concentration was kept constant for other experiments performed in the study. Another point to be noted is that in the case of the indirect measurement, there is still a considerable signal from BSA-FITC even in the plateau regime of the curve, indicating that a monolayer condition is not reached and there still exists enough free space on the surface for the BSA-FITC binding. Although the studies have been performed on PDMS microstructures sealed to a glass substrate, the results can be extended to PDMS substrates as well, since the surface coverage for these two surfaces is comparable in terms of the signal obtained (ESI, Fig. S1†). From this analysis it can be concluded that while the physisorption based strategy is versatile and easy to perform, it tends to require higher concentrations of the capture antibody to achieve comparable surface densities, in comparison with previously reported chemical based[40] or affinity based[24] strategies with concentrations in the range of 4–16 or 2 ng mL^{-1} respectively. Nevertheless, for immunoassays developed in microfluidic environments, the reagent volumes required per analysis should compensate for this limitation in terms of cost.

Relative surface coverage of the immobilised probe. Nanospotting was used to determine the relative surface coverage of the immobilised probe on the surface. This method was chosen as it is robust and allows precise deposition of a controlled volume and amount of Abs on the surface using a computer-controlled spotter.[38] The antibody is loaded on a nano- or a pico-tip that creates spots on the surface by dispensing the solution in a non-contact mode, thus allowing the fabrication of the desired matrix of precisely placed Ab spots using volumes of solutions in the nL or pL range. Calibration of FITC-labelled α-mouse IgG by fluorescence microscopy was used for determining the surface density of the adsorbed Abs. Labelled α-mouse IgGs were spotted in the microchannel at varying concentrations. The fluorescence resulting from FITC labels was measured in the spotted areas and the total number of Abs immobilised (by physical adsorption) per unit area was then calculated (a correlation between the total number of IgGs in the spot and the intensity from the spot can be determined, as the initial concentration of the Ab in solution and the spotted volume are known). In addition, a linear dependence of the average fluorescence intensity as a function of the spotted antibody concentration can also be obtained (ESI, Fig. S2†). Fig. 2 shows the correlation between the fluorescence signal measured in the spots and the relative surface coverage of α-mouse Abs, which can be used to estimate the surface density of the molecules used in the PSA-specific experiments. The inset in Fig. 2 and the associated dotted lines show the relative surface coverage values when PSA-specific Ab such as Ab178776 is used, at the same concentration optimized in the previous section. The microchannel was prepared according to flow conditions described in the Methods section and the inset image shows only one surface of the structure. The surface density values are in agreement with those obtained by Novo *et al.*,[38] using the same α-mouse Abs, where it has been suggested that the experimental saturation value of the probe Ab surface density is at 30% of its maximum capacity. The

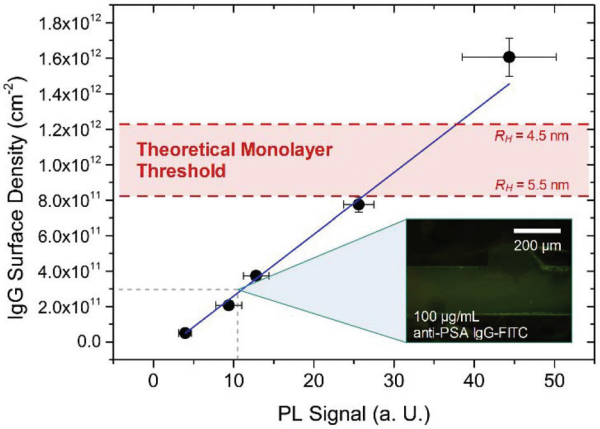

Fig. 2 Nanospotting of α-mouse IgGs to estimate the surface density. A correlation between the photoluminescence (PL) signal obtained using the microscope and the IgG surface density is established from the nanospotting experiment. The inset figure shows the optical micrograph of a microchannel adsorbing FITC labelled α-PSA antibody at 100 µg mL^{-1}. The dotted lines relate to the PL signal obtained from the channel and the corresponding surface coverage. The shaded region represents the calculated theoretical monolayer threshold for IgGs on the surface.

spotted area is estimated at ~2.3×10^{-4} cm^2. The calculated area occupied by a single Ab molecule, assuming a hydrodynamic radius (R_H) of 5 nm, gives an area of ~9.5×10^{-13} cm^2; this surface area occupied by the Ab, although dependent on its orientation, could be enhanced for increased adsorption using appropriate surface chemistries. A theoretical monolayer threshold, based on the Ab dimensions and obtained spot areas, is also indicated in Fig. 2, where the shaded region corresponds to a threshold band, considering the possible upper and lower limits for the hydrodynamic radii relevant for Abs.[41] Enhancements either by engineering the Abs for increased adsorption[20] or by employing suitable strategies (physical, chemical or kinetic) to tailor the immobilisation[33,34] might help in moving towards this threshold band even at relatively low concentrations in solutions.

After establishing the relationship between the surface density and the corresponding fluorescence signal, the anti-PSA (α-PSA) Ab spotted microchannels were sealed using corona and a complete sandwich experiment was performed. The α-PSA antibody was spotted using the optimized humidity (60%) and glycerol (5%, v/v) conditions and a clear difference between the control (containing no PSA) and the sample (containing 100 ng mL^{-1} of PSA) was noticed (ESI, Fig. S3†). The sealing was performed using the corona method and not UVO as for the other experiments, in order not to destroy the spotted proteins in the open microchannel. By using the corona discharge treater, the electrical discharge can be directed away from the spots while with UVO, the full channel would be exposed to the UV ozone. Nevertheless, corona and UVO sealing result in the same final absolute signal after adsorbing FITC labelled antibodies under flow conditions, thus providing comparable surface densities (ESI, Fig. S4†).

Optimisation controls for fPSA detection

Before performing the complete fPSA assay, the individual steps in the microfluidic assay were checked for specificity and cross-reactivity, both being critical parameters when using an immunoassay for biomedical detection.[35] Fig. 3 summarises the control experiments for fPSA assay.

Fig. 3 shows that when only the probe Ab was adsorbed on the surface, there was no signal from the microchannel upon flowing of the substrate (1) as there is no chemiluminescent tag attached to the molecule, while the adsorption of only the detector Ab labelled with HRP shows an elevated signal as seen in (2). When the surface was blocked with BSA and then the HRP-labelled detector is flowed, the microchannel showed almost no signal (3), comparable to that obtained in (1), indicating effective blocking. The blocking molecule (such as BSA alone or casein alone or a mixture of both) as well as the time of incubation of the blocking molecule in the microchannel (5 min or 10 min) do not influence the final signal (ESI, Fig. S5†). Hence, 4% BSA flowed for 5 min, to reduce the overall assay time, was chosen as the appropriate blocking condition for the microfluidic immunoassays. After checking the blocking effect, the signal resulting from non-specific adsorption was checked. For this, the capture molecule was adsorbed on the surface, followed by the HRP-labelled detector Ab, without any blocking in between. As expected, this gave rise to a high signal (4) corresponding to the non-specific adsorption of the detector molecules in the free space available in the microchannel, both on the sensing surface as well as to the walls of the microchannels, in the absence of blocking. However, when a blocking step is introduced between the flow of the capture and the detector Ab molecules, the signal is drastically reduced (5), being only slightly higher than that in (3). This signal from (5) also corresponds to the signal arising due to the cross-reactivity between the capture and the detector Ab molecules used in the study. A complete sandwich experiment, with the capture Ab adsorbed on the surface, followed by blocking, then flowing the analyte and finally the detector Ab molecule, with intermittent washing at the end of every step, was performed to establish the difference between the control (zero concentration) (6) and a finite concentration of the analyte (7). The slightly higher signal in (6), which is basically the same assay as (5) but with an extra 10 min of washing (0 ng mL^{-1} PSA corresponds to just flowing PBS buffer), suggests the possibility of erosion of certain molecules (including BSA) upon prolonged incubation. In this context, incubation and flow rate become critical for an immunoassay, and in the current study the capture and detector Ab molecules, as well as the analyte are flowed at a rate of Q = 0.5 μL min^{-1} for 10 min, with intermittent PBS wash at a tenfold higher flow rate for a minute. Tests were conducted to confirm whether or not there is erosion of certain molecules during the incubation and washing steps. It was observed that while the drop in fluorescence for microchannel surface adsorbed anti-mouse FITC and BSA-FITC was negligible for the relatively short times of washing used (4 min), after 55 min of incubation, the fluorescence of anti-mouse FITC drops approximately 20%, while the BSA-FITC remains unaffected (ESI, Fig. S6†). The flow rate for blocking remains the same as that of the other molecules, but with half the incubation time, namely 5 min as described before (ESI, Fig. S5†).

In addition to the flow rate and incubation time that play a key role in the microfluidic surface reactions,[42] attention needs to be paid to the washing steps, as inadequate washing might result in a non-specific signal from weakly bound molecules and excessive washing might result in the erosion of the desired molecules, as described previously. In addition, the buffer used for washing also becomes relevant, as the salt content and concentration influence the adsorption and subsequent reactions, governed by the charge overcompensation

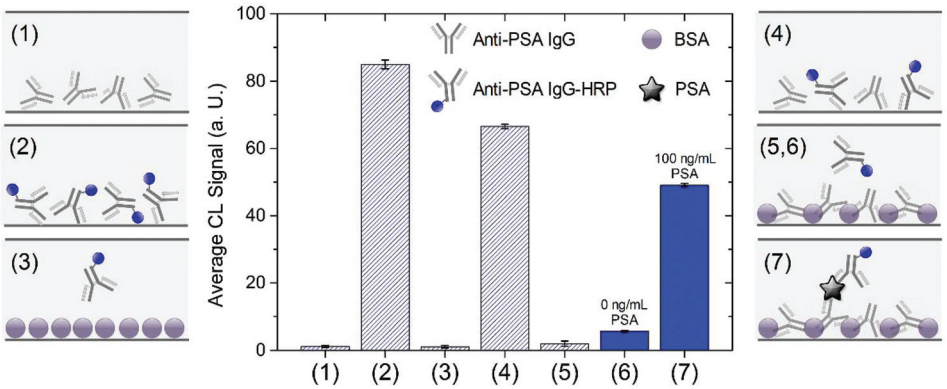

Fig. 3 Optimisation of fPSA detection by systematically delineating the individual assay steps. (1) Adsorption of probe α-PSA Ab (Ab10187) on the surface. (2) Adsorption of detector α-PSA Ab-HRP (Ab24466) on the surface. (3) Blocking the surface with 4% BSA, followed by the adsorption of detector α-PSA Ab-HRP. (4) Check for non-specific adsorption by flowing the probe antibody and then the detector antibody used for the fPSA assay. (5) Cross-reactivity check between the capture and detector antibodies, by the adsorption of capture α-PSA Ab, followed by BSA blocking and then flowing detector α-PSA Ab-HRP. (6) A sandwich experiment with 0 ng mL^{-1} of fPSA. (7) A sandwich experiment with 100 ng mL^{-1} of fPSA, represented as a star – sandwiched between the capture and detector antibody.

and masking effects.[27,43] In this study, PBS with a phosphate ion concentration of 10 mM was used for both dilution and washing of the molecules (ESI, Fig. S7†). The pH of the solutions was maintained under neutral conditions, as for PSA-specific Abs, the highest antigen binding efficiency was reported close to neutral pH, hence proving critical for molecular recognition.[27] Next, stringent specificity is crucial to ensure accurate discrimination among the abundance of biomolecules found in a sample.[30] To check the specificity of the molecules used for the chosen immunoassay, IL6, a cytokine and another promising biomarker for PCa, also detected in serum,[1,44] and IL6-specific Abs were stringently chosen. It was noticed that neither the fPSA Ab cross-captured the IL6 nor was the fPSA detected using IL6-specific Abs (ESI, Fig. S8†), thus validating the specificity of the chosen analyte–Ab pairs.

Fig. 4 shows the effect of a biological matrix on the signal obtained from a fPSA sandwich experiment. Since the assays, when extended to PoC, would require measurements in biological matrices, experiments were performed with a 4% human serum albumin (HSA) solution (since human serum contains albumin as the major constituent protein) to compare with the spiked buffer solutions. As can be seen from the graph, the ratio of the signal from the sample, corresponding to 100 ng mL^{-1} of fPSA, to that of the control remains almost the same for both the PBS and HSA tests. The observed drop in the absolute chemiluminescence value might be related to the higher viscosity inherent to increased albumin concentrations, which may pose constraints to the effective diffusivity of the PSA molecules from the bulk of the solution to the surface of the microchannel. Nevertheless, based on the similarities in the obtained ratios, the actual assays were further conducted in solutions with fPSA spiked in PBS.

Bio-affinity amplification-based fPSA detection

After optimizing the assay parameters using a systematic approach, the goal was to detect fPSA in a clinically relevant range using the microfluidic sandwich immunoassay. Fig. 5 summarises the assay design and the results obtained for fPSA detection. (I) represents the sandwich assay without amplification, where the analyte is captured between the probe (Ab10187) and the detector Ab (Ab24466). The results of this approach are represented in Fig. 1 by the open circles. The LoD of this approach was approximately 21.4 ng mL^{-1}, slightly above the 'gray zone' (4–20 ng mL^{-1}) of the clinical regime.[1,37] Hence, it was necessary to push down the values of LoD in order to be able to detect lower levels of fPSA that could be used in PCa diagnostics.

To achieve lower values of LoD with this sandwich assay, we developed an amplification strategy to be employed at the detector end of the assay. The bio-affinity of streptavidin–biotin was exploited for this purpose, thanks to the high specific activity of streptavidin that helps in improving the assay sensitivity. When the analyte is captured by the immobilised probe Ab, instead of directly detecting the captured analyte using a labelled detector Ab (such as Ab24466 or Ab178776), we introduced a network of streptavidin and biotin that binds to the biotinylated detector Ab specific for PSA (such as Ab182031 or Ab182030). In this assay, we used a network comprising of pre-incubated unlabelled streptavidin and biotinylated BSA (owing to the very small molecular weight of biotin, a conjugated version was employed for the assay), which is then bound to HRP-labelled streptavidin to enable chemiluminescence detection. Based on the high affinity of the streptavidin–biotin complex as well as on the high number of biotin binding sites available in the network, a considerable decrease in the LoD with such amplification was noticed. In Fig. 5, the triangles show that using the amplification strategy with Ab10187 as capture Ab, an LoD of 5 ng mL^{-1} could be reached (although with a high background signal); with a change in capture Ab to Ab10185 (stars in Fig. 5), the LoD value was further decreased to 2.7 ng mL^{-1}, thus approaching the clinical window for PSA detection. Interestingly, our previous studies with SPR for a sandwich immunoassay model using the same set of antibodies indicate that despite nearly identical dissociation constants for both Ab10187 and Ab10185, kinetic parameters of binding revealed a ten-fold higher k_{on} and a ten-fold lower k_{off} for Ab10185.[45] Thus, in principle, Ab10185 should yield lower LoD values than Ab10187 when used in a sandwich assay to capture the analyte, and this is indeed what is observed in the present results (with an almost 50% reduction in LoD with Ab10185 compared to Ab10187). On the whole, the associated changes in kinetic properties of the molecules used and the assay design (with systematic optimisation of the surface as well as microfluidic parameters) brought a ten-fold decrease in LoD. The decrease of the LoD using an altered Ab also suggests at the potential of further gains in sensitivity with Ab engineering based on their kinetic parameters.[20,33] Furthermore, the critical importance of surface engineering must be balanced with the considerations of the kinetics of the chosen molecules to maximise molecular recognition and biosensor sensitivity.

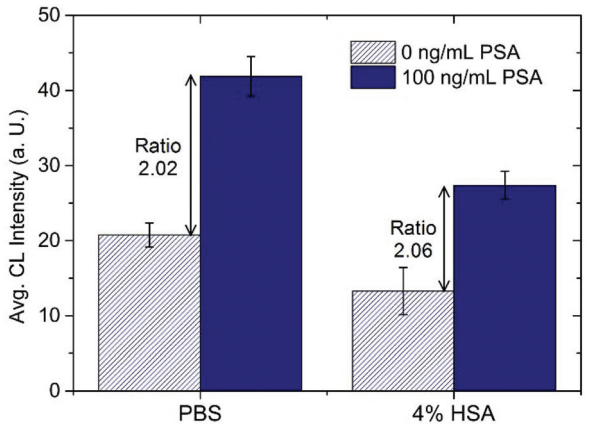

Fig. 4 Matrix effect. Measurements of fPSA, along with the control, spiked in PBS and 4% human serum albumin. The ratio of the sample to the control remains almost a constant in both the buffer and the matrix solutions.

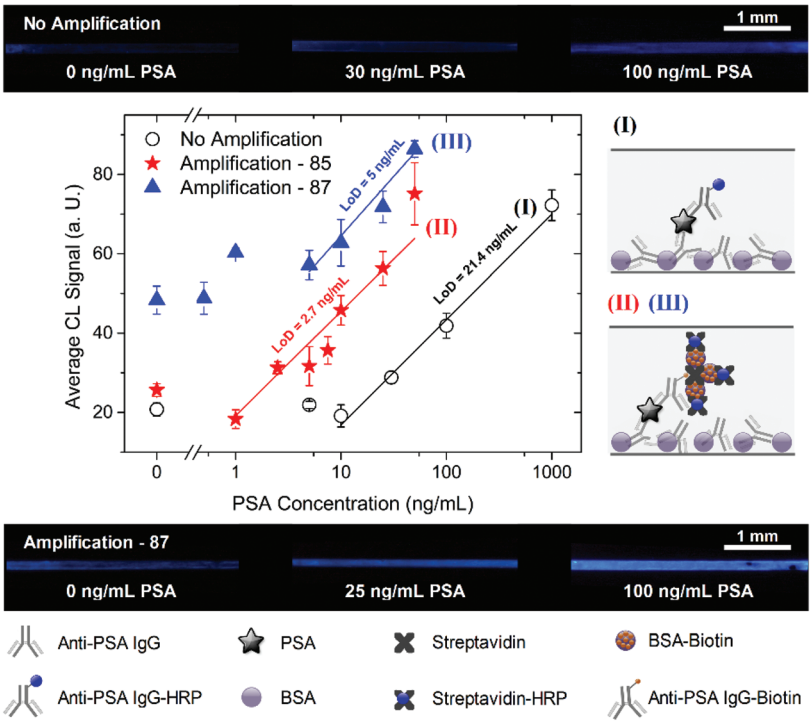

Fig. 5 Measurement of fPSA using a microfluidic sandwich immunoassay. (I) shows chemiluminescence measurements without amplification, where PSA is captured between the probe and the detector antibodies. To bring down the values of the obtained LoD, methods (II) and (III) were tried with two different capture antibodies, namely Ab10185 and Ab10187, respectively. (II) and (III) involve capturing of PSA by the immobilised probe antibody, followed by detection using a biotinylated antibody (Ab182031). The signal generation was achieved by using a network of unlabelled streptavidin→biotin labelled BSA→HRP labelled streptavidin, and flowing luminol in the microchannel. The channels were blocked with BSA in all the cases. The optical micrographs of the microchannels for varied PSA concentrations, upon luminol flow, are also shown for visual comparison of the light intensities obtained. (Note that the schematic for (II) and (III) show biotinylated BSA (coupled to HRP labelled streptavidin molecules) attached to only single unlabelled streptavidin for clarity purposes; however, in reality, this is a larger network as described in the text).

Although one could consider that increasing the chain in this network would be expected to further enhance the signal, in this work, we chose not to increase the number of steps for two main reasons: (i) we were already able to reach the clinically relevant regime; and (ii) minimizing the assay time is an important consideration in developing a device for PoC applications. The parameters for signal acquisition were optimized and summarized in the ESI (Table S1†) and these optimized conditions were used for the signal generation and acquisition, reflecting on the fact that the established difference in the signal noticed for such lower limits of analyte results from the molecular events only and not any redundancy or noise from the signal measurement process.

Implications of surface kinetics and probe density in the microfluidic assay

To have a clear picture of what happens in a surface-based assay, it is critical to understand how the various parameters (inherent and derived) contribute to the over-all assay performance.

Table 3 shows the physical and chemical parameters calculated for the immunoassay described above and the corresponding inference from the values obtained. From Table 2, it is possible to conclude that the immunoassay is performed under reaction limited conditions, where most of the analyte molecules are swept downstream and not captured. This is a consequence of the high Peclet number. When equilibrium conditions are achieved, only a small fraction of the number of probes is occupied, which is a direct consequence of the target analyte concentration being more than one order of magnitude below the K_d of the probe. Thus, the optimization of such physical and chemical parameters would help in achieving higher levels of sensitivity.[30] For instance, from the above table, altering the b_{eq} by changes made either to the probe surface density b_m (by suitable surface engineering strategies) or to the kinetic parameter such as K_d (by antibody engineering) would result in a simulated plot as shown in Fig. 6. Surface engineering strategies range from classical covalent chemistry to the recent use of 3D surfaces for enhanced adsorption[46] and antibody engineering focuses on improvising the orientation and confirmation of Abs on sensor surfaces.[32]

For a 2D surface, using engineered Abs with increased K_d (or using high affinity tags like biotin–streptavidin) to allow reaching high probe saturation up to the maximum theoretical monolayer threshold, the simulation yields an appreciable gain in sensitivity, without any compromise in the dynamic

Table 3 Optimisation and associated assay conditions for fPSA detection[a]

Parameter	Value	Notes
(a) Physical		
Pe_H	490	Peclet number relative to the channel height ($Pe_H \gg 1$ indicates that $\delta_s \ll H$)
Pe_S	6.62×10^7	Peclet number relative to the sensor ($Pe_S \gg 1$ indicates that $\delta_s \ll L$)
F	404	Sherwood number ($F < Pe_H$ indicates that analyte molecules are swept downstream without effective diffusion in H)
J_D	6.34×10^5 s^{-1}	Total flux, relates to the total number of analyte molecules impinging the sensor per unit time
(b) Chemical		
Da	0.055	Damköhler number (Da $\ll 1$ indicates a reaction limited regime, rather than a mass transport limitation)
C'	0.009	$C_o/K_d \ll 1$ indicates that only a small fraction of the probes is bound to the analyte molecules in equilibrium
b_{eq}	1.31×10^9 cm^{-2}	Density of probes bound to analyte molecules in equilibrium
b_{eq}/b_m	0.87%	Fraction of the probes occupied by analyte molecules in equilibrium
N_R^B	7.87×10^6	Effective number of probes bound to analyte molecules in equilibrium
τ_R	3.75 min	Time to reach equilibrium conditions in a reaction-limited regime

[a] Assuming the detection of 4 ng mL^{-1} (153 pM) PSA in solution. δ_s refers to the thickness of the PSA depletion zone above the sensing area.

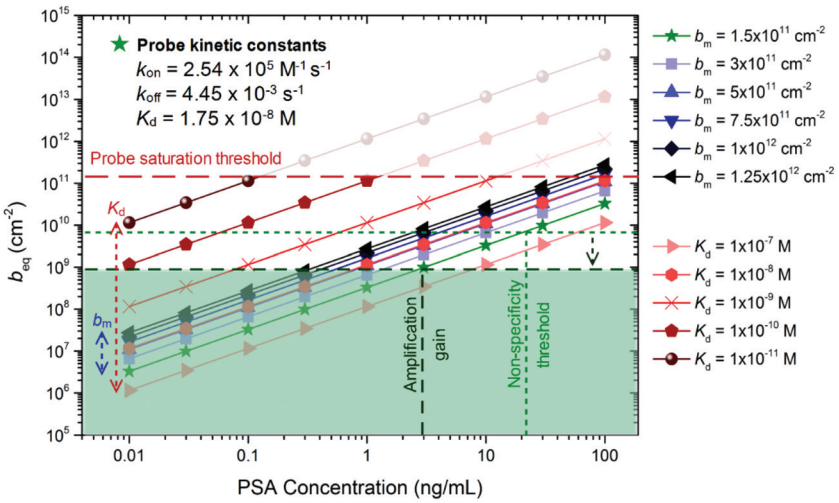

Fig. 6 Simulated b_{eq} plot for varied b_m and K_d for different PSA concentrations. The K_d values were derived by fixing the b_m (experimental conditions) as indicated by a star. Kinetic parameters represented are for the capture antibody Ab10185.

range measured. However, it can be noticed from the plot that when using novel engineered binding proteins[47] or peptide aptamers[48] or affimers (non-Ab binding proteins) with very low K_d (*e.g.*, $\ll 1 \times 10^{-11}$ M), altering only the K_d would cause the system to become ultra-sensitive, resulting in a saturated signal (indicated by $b_{eq} = b_m$) even within the clinical range (for example, PSA values higher than 0.1 ng mL^{-1} would yield saturated signal for the described conditions from the plot). On the other hand, manipulating the b_m alone by altered surface densities, which is more practical and simpler from an experimental point of view, would serve as a potential alternative, however with inherent limitations on the monolayer threshold as well as the dynamic working range. Fig. 6 also suggests that the gain in amplitude for the fraction of probes bound in equilibrium to the analyte is higher than the gain in signal amplitude obtained by changing only the b_m (indicated in Fig. 6 by double arrows K_d and b_m, respectively). Although this discussion has been made for the capture Ab, the same argument also holds true for the detector Ab.

Fig. 6 also details upon some conclusions to be drawn about the threshold limits of the sensing *per se.* For instance, it becomes evident that when there is probe saturation along with a very small K_d, sample dilution might serve as an alternative for measurements in the desired lower ranges. Use of a system with an increased number of HRP molecules (for example, as resulting from the amplification experiments) or enhanced probe adsorption might lead towards gain in b_{eq}, thus aiding the detection. In practice, such amplification mechanisms result in a broadening of the dynamic range, as shown in Fig. 6 as the difference between the non-specificity threshold and the amplification gain. One can intuitively account for this gain as a virtual decrease in detectable b_{eq}, emerging from having more than one HRP molecule per probe molecule on the surface. Thus, the whole assay scenario is

noticed as a close interplay and balance-seeking approach between the surface and the kinetic parameters.

Conclusion

We present a novel, simple, passive adsorption-based diagnostic immunoassay with bio-affinity amplification as a potential platform for PoC analysis of PCa biomarkers, with fPSA as the model system. This platform is generic and can be extended to other biomarkers,[1] and can also be developed into a multiplexed diagnostic system. We highlight this system as a simple systematic and quantitative approach, with potential to effectively measure the clinical range for PSA, avoiding the need for complex assay designs or chemistry and economizing reagent usage. Using the appropriate optimization of surface chemistry and microfluidics, the LoD was brought down to 21.4 ng mL^{-1} and, upon an additional amplification strategy the system yielded a further 10-fold reduction in LoD (2.7 ng mL^{-1}), effectively reaching the clinical grey zone. Our results highlight the importance of a systematic optimisation, starting from the simplest and fastest means of performing the assay and integrating relevant amplification mechanisms, to reach the desired sensitivity. The current study can potentially be extended to tPSA measurement and performance of the immunoassay in a complex biological matrix containing a mixture of proteins, integrating data acquisition on the chip,[37] and using a colorimetric mode of detection for a 'sample-in, answer-out' PoC tool for PCa. In short, this study took a systematic, multidisciplinary approach towards the optimization of both surface and microfluidic parameters and coupled this with enhancement strategies (such as the bio-affinity based amplification) to demonstrate a potential simple system of a point-of-care device for diagnostic and monitoring purposes.

Acknowledgements

The authors wish to thank Eduardo Brás for performing the substrate and salt optimization experiments. N. Madaboosi acknowledges Dr Sofia Martins for her fruitful and effective contribution to the brainstorming session about the immunoassays. N. Madaboosi acknowledges the Marie Curie ITN PROSENSE for a fellowship and R. Soares acknowledges Fundação para a Ciência e a Tecnologia (FCT) for a PhD grant (SFRH/BD/97354/2013). The authors wish to thank the Marie Curie ITN for funding and FCT for funding through the Associated laboratory IN and through the research project EXCL/CTM-NAN/0441/2012.

References

1 V. M. Velonas, H. H. Woo, C. G. Remedios and S. J. Assinder, *Int. J. Mol. Sci.*, 2013, **14**, 11034–11060.
2 G. Ploussard, J. I. Epstein, R. Montironi, P. R. Carroll, M. Wirth, M. O. Grimm, A. S. Bjartell, F. Montorsi, S. J. Freedland, A. Erbersdobler and T. H. van der Kwast, *Eur. Urol.*, 2011, **60**, 291–303.
3 A. B. Reed and D. J. Parekh, *Expert Rev. Anticancer Ther.*, 2010, **10**, 103–114.
4 S. F. Shariat, A. Semjonow, H. Lilja, C. Savage, A. J. Vickers and A. Bjartell, *Acta Oncol.*, 2011, **50**(Suppl 1), 61–75.
5 M. Kuriyama, Y. Kawada, Y. Arai, H. Maeda, S. Egawa, K. Koshiba, K. Imai and H. Yamanaka, *Jpn. J. Clin. Oncol.*, 1998, **28**, 661–665.
6 F. H. Wians Jr., C. D. Cheli, J. A. Balko, D. J. Bruzek, D. W. Chan and L. J. Sokoll, *Clin. Chim. Acta*, 2002, **326**, 81–95.
7 X. Filella and N. Giménez, *Clin. Chem. Lab. Med.*, 2013, **51**, 729–739.
8 J. T. Wu and L. W. Wilson, *J. Clin. Lab. Anal.*, 1995, **9**, 252–260.
9 H. Yu and E. P. Diamandis, *Clin. Chem.*, 1993, **39**, 2108–2114.
10 O. Karim, A. Rao, M. Emberton, D. Cochrane, M. Partridge, P. Edwards, I. Walker and I. Davidson, *Prostate Cancer Prostatic Dis.*, 2007, **10**, 270–273.
11 S. W. Oh, Y. M. Kim, H. J. Kim, S. J. Kim, J.-S. Cho and E. Y. Choi, *Clin. Chim. Acta*, 2009, **406**, 18–22.
12 G. Posthuma-Trumpie, J. Korf and A. van Amerongen, *Anal. Bioanal. Chem.*, 2009, **393**, 569–582.
13 P. Huhtinen, T. Soukka, T. Lovgren and H. Harma, *J. Immunol. Methods*, 2004, **294**, 111–122.
14 R. Wiese, Y. Belosludtsev, T. Powdrill, P. Thompson and M. Hogan, *Clin. Chem.*, 2001, **47**, 1451–1457.
15 G. Wu, R. H. Datar, K. M. Hansen, T. Thundat, R. J. Cote and A. Majumdar, *Nat. Biotechnol.*, 2001, **19**, 856–860.
16 G. M. Whitesides, *Nature*, 2006, **442**, 368–373.
17 E. K. Sackmann, A. L. Fulton and D. J. Beebe, *Nature*, 2014, **507**, 181–189.
18 T. Das and S. Chakraborty, *Biomicrofluidics*, 2013, **7**, 11811.
19 D. A. Healy, C. J. Hayes, P. Leonard, L. McKenna and R. O'Kennedy, *Trends Biotechnol.*, 2007, **25**, 125–131.
20 P. J. Conroy, S. Hearty, P. Leonard and R. J. O'Kennedy, *Semin. Cell Dev. Biol.*, 2009, **20**, 10–26.
21 A. I. Barbosa, A. P. Castanheira, A. D. Edwards and N. M. Reis, *Lab Chip*, 2014, **14**, 2918–2928.
22 M. Ikami, A. Kawakami, M. Kakuta, Y. Okamoto, N. Kaji, M. Tokeshi and Y. Baba, *Lab Chip*, 2010, **10**, 3335–3340.
23 A. A. Tajudin, K. Petersson, A. Lenshof, A. M. Sward-Nilsson, L. Aberg, G. Marko-Varga, J. Malm, H. Lilja and T. Laurell, *Lab Chip*, 2013, **13**, 1790–1796.
24 J. L. Garcia-Cordero and S. J. Maerkl, *Lab Chip*, 2014, **14**, 2642–2650.
25 R. Malhotra, V. Patel, B. V. Chikkaveeraiah, B. S. Munge, S. C. Cheong, R. B. Zain, M. T. Abraham, D. K. Dey, J. S. Gutkind and J. F. Rusling, *Anal. Chem.*, 2012, **84**, 6249–6255.
26 R. S. Sista, A. E. Eckhardt, V. Srinivasan, M. G. Pollack, S. Palanki and V. K. Pamula, *Lab Chip*, 2008, **8**, 2188–2196.

27 X. Zhao, F. Pan, L. Garcia-Gancedo, A. J. Flewitt, G. M. Ashley, J. Luo and J. R. Lu, *J. R. Soc., Interface*, 2012, **9**, 2457–2467.
28 M. Wilchek and E. A. Bayer, *Biomol. Eng.*, 1999, **16**, 1–4.
29 H. Härmä, T. Soukka and T. Lövgren, *Clin. Chem.*, 2001, **47**, 561–568.
30 S. O. Kelley, C. A. Mirkin, D. R. Walt, R. F. Ismagilov, M. Toner and E. H. Sargent, *Nat. Nanotechnol.*, 2014, **9**, 969–980.
31 M. E. Wiseman and C. W. Frank, *Langmuir*, 2012, **28**, 1765–1774.
32 A. K. Trilling, J. Beekwilder and H. Zuilhof, *Analyst*, 2013, **138**, 1619–1627.
33 T. M. Squires, R. J. Messinger and S. R. Manalis, *Nat. Biotechnol.*, 2008, **26**, 417–426.
34 S. C. Gopinath, T. H. Tang, M. Citartan, Y. Chen and T. Lakshmipriya, *Biosens. Bioelectron.*, 2014, **57**, 292–302.
35 C.-C. Lin, J.-H. Wang, H.-W. Wu and G.-B. Lee, *J. Lab. Autom.*, 2010, **15**, 253–274.
36 R. R. Soares, P. Novo, A. M. Azevedo, P. Fernandes, M. R. Aires-Barros, V. Chu and J. P. Conde, *Lab Chip*, 2014, **14**, 4284–4294.
37 N. Madaboosi, C. R. Pedrosa, M. F. Reis, R. R. G. Soares, V. Chu and J. P. Conde, *IEEE Sensors Proceedings*, 2014.
38 P. Novo, D. M. Prazeres, V. Chu and J. P. Conde, *Lab Chip*, 2011, **11**, 4063–4071.
39 A. Belanger, H. van Halbeek, H. C. Graves, K. Grandbois, T. A. Stamey, L. Huang, I. Poppe and F. Labrie, *Prostate*, 1995, **27**, 187–197.
40 C. Xie and G. Wang, *J. Clin. Lab. Anal.*, 2011, **25**, 37–42.
41 D. Bethea, S. J. Wu, J. Luo, L. Hyun, E. R. Lacy, A. Teplyakov, S. A. Jacobs, K. T. O'Neil, G. L. Gilliland and Y. Feng, *Protein Eng., Des. Sel.*, 2012, **25**, 531–537.
42 N. Madaboosi, K. Uhlig, M. S. Jäger, H. Möhwald, C. Duschl and D. V. Volodkin, *Macromol. Rapid Commun.*, 2012, **33**, 1775–1779.
43 R. A. Latour, in *Encyclopedia of Biomaterials and Biomedical Engineering*, 2005, pp. 270–284, DOI: 10.3109/9781420078039.026.
44 B. Bickers and C. Aukim-Hastie, *Anticancer Res.*, 2009, **29**, 3289–3298.
45 P. Damborský, N. Madaboosi, V. Chu, P. Conde João and J. Katrlík, in *Chemical Papers*, 2015, vol. 69, p. 143.
46 D. Kim and A. E. Herr, *Biomicrofluidics*, 2013, **7**, 41501.
47 H. K. Binz, P. Amstutz and A. Pluckthun, *Nat. Biotechnol.*, 2005, **23**, 1257–1268.
48 R. Woodman, J. T. H. Yeh, S. Laurenson and P. K. Ferrigno, *J. Mol. Biol.*, 2005, **352**, 1118–1133.